



## Original Research Article

### Tripping Zone Accuracy of Distance Relay Protection for a 33 kV Distribution System with Varying Fault Type and Impedance

\*<sup>1</sup>Oputa, O., <sup>2</sup>Ogbuka, C.U., <sup>1</sup>Diyoke, G.C., <sup>1</sup>Onwuka, I.K. and <sup>2</sup>Madueme, T.C.

<sup>1</sup>Department of Electrical/Electronic Engineering, Michael Okpara University of Agriculture, Umudike, Nigeria.

<sup>2</sup>Department of Electrical Engineering, University of Nigeria, Nsukka, Nigeria.

\*connectositao@gmail.com

<http://doi.org/10.5281/zenodo.10442845>

#### ARTICLE INFORMATION

##### Article history:

Received 14 Oct. 2023

Revised 12 Dec. 2023

Accepted 14 Dec. 2023

Available online 30 Dec. 2023

##### Keywords:

Trip zone accuracy

Distance relay

Varying fault type

Varying fault impedance

Distance protection

#### ABSTRACT

*The zone at which a Distance protection scheme (DPS) trips when a fault occurs on a line the DPS is protecting is ideally thought to be just dependent on the location at which the fault occurred. However, it has been shown in this paper through simulations in PSCAD that the trip location depends on not only the fault location but also depend on the fault impedance, type of fault and the phase(s) involve in the fault. The PSCAD simulation of an impedance fault of  $0.1 \Omega$  occurring at 50 km (Zone 1) on Line 1 for a line 'A' to ground fault (AG) trips inaccurately at Zone 2 while for a BG fault, it trips accurately at Zone 1. Also, line 'A' to line 'C' fault at the same location trips at Zone 1 for fault impedances of  $0.1 \Omega$  and  $1 \Omega$ . The same fault at the same location across the same line trips in Zone 2 and Zone 3 for fault impedance of  $5 \Omega$  and  $10 \Omega$  respectively. This buttress the fact about the trip zone stated above. Also, test carried out shows an average tripping zone accuracy of the distance relay of 62.5 %.*

© 2023 RJEES. All rights reserved.

## 1. INTRODUCTION

Fault occurrence on power distribution systems pose a great challenge to power system protection engineers. The overcurrent relay and protection system were developed to protect the power system and its components. In this protection system, the time dial setting (TDS) determines the actual operating time of the relay while plug setting multiplier (PSM) determines the required amount of current values with which the relay is to pick up. However, finding optimum values of TMS and PSM of this relay must be well coordinated, else the relay may malfunction. Different algorithm/optimization techniques have been put forward to obtain optimal TDS and PSM of the relays. This include the JAYA algorithm and the simplex method firefly algorithm (Noghabi et al 2009; Bedekar et al., 2010; Pragati and Amol 2017), nature – inspired root tree algorithm and

the bacterial foraging algorithm (a natural and biological model), (Adhikari and Sinha 2016; Wadood et al., 2018). However, the fact that the operating time and pick up values of the overcurrent relays depend on the fault current which varies with the fault type and circuit characteristics, the overcurrent relay and protection scheme was less attractive in protecting high voltage systems (grids) where different power plants and load centers are interconnected. This is because any malfunction of this relay may cause instability in the concerned grid.

This led to the emergence of the distance relays and protection scheme which operates when the impedance seen by the relay is less than the predetermine/set impedance of the relay. The relay calculates the seen impedance by extracting the voltage and current from the complex post – fault waveforms (Murthy 2007). Different algorithms have been put up by different researchers in extracting the voltage and current from the complex post – fault waveform. The fast Fourier transform algorithm with full cycle window to remove the DC offset value (contained in power line fault current) and to obtain the fundamental component of the current and voltage signals by using a microcontroller (Verma and Sinha 2016). However, this algorithm presents a compensation matrix in the frequency domain which reduces the accuracy current and voltage signal extraction which is a major setback in the algorithm. The least squares matrix pencil algorithm of extracting the complex fault current and voltage waveform parameters makes use of the function model that makes square fitting (Suonan et al., 2010). However, under this condition the function model of the input signal is given in advance which stands as a strong problem of this algorithm. Fast phasor calculation algorithm was also pulsated. This algorithm uses the matrix pencil method in extracting the fault current and voltage waveform (Huanhuan et al., 2014).

In the past, different composition of the distance protection has been put forward. For example, a directional comparison distance protection scheme using average superimposed components of voltage and currents has been proposed (Hashemi et al., 2013). The current and voltage values are approximately zero under the normal operating condition and none zero value during a fault. The algorithm provides fast fault detection in less than half cycle time and almost 100 % coverage of the line. However, this approach suffers from inherent inaccuracy due to the application of the R – L (resistance – inductance) type line model and complexity in protection criterion. A technique for transmission line protection scheme based on alienation coefficients for current signals was also developed (Masoud and Mahfouz 2010). The fault selection algorithm is based on alienation technique of two half successive cycles with the same polarity and used only three lines current measurement available at the relay location. This algorithm was purely for transmission system containing just one transmission line linking two buses alone. An impedance differential protection scheme for pilot protection of transmission lines using the voltage and currents of both local and remote ends to calculate the differential impedance (Ghanizadeh et al., 2015). The proposed scheme is capable of fast discrimination between internal and external faults and eliminates the problem of line capacitive charging current and source impedance strength which are the challenges of the conventional scheme. However, the scheme requires a reliable communication channel for data transmission. A pilot distance protection scheme based on the fault component integrated power was used as a criterion for discrimination between internal and external faults was developed by (Tohid et al., 2014). As the integrated power is a sum of active powers which are injected into the transmission line from both ends, the integrated power is divided into pre-fault and post fault powers and the difference between the two values is called the faulty component. When there is a fault, the pre-fault power is equal to the active losses of lines while fault component integrated power is equal to zero. But when a fault occurs, it changes from its zero value to a non – zero value. The method is able to quickly discriminate the normal condition, internal fault and external fault. A high speed power line protection scheme was proposed using High – Speed Directional and fault Type Selection (HSD-FTS) algorithm (Benmouyal et al 2004). This used a high speed distance element which is a logical system for its operation. This algorithm prevents zone 1 element overreach especially in series compensated transmission lines. How the distance protection scheme of an 11 kV distribution scheme behaves with varying fault impedance have been revealed by (Onwuka et al., 2023).

Despite all these research works carried out on the distance relay and DPS, the accuracy at which these relay trip in their protective zones with varying fault impedance, fault type and phase(s) involved in the fault have not being examined. Hence, this paper investigates this for a 33 kV power distribution system.

## 2. MATERIALS AND METHODS

### 2.1. Model Development

In this section, the mathematical model of the Distance Relay/Protection Scheme of a 33 kV distribution line shall be develop. Consider the 3 phase line shown in Figure 1 with voltage  $E_a, E_b,$  and  $E_c$  for the 3 phases and  $I_a, I_b,$  and  $I_c$  are the current flowing in the phases respectively with line impedance  $Z$ .

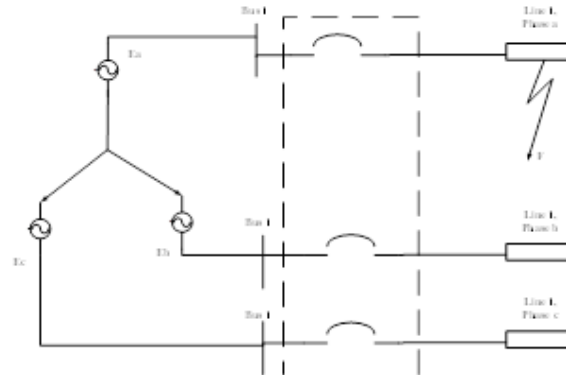


Figure 1: Three phase line with fault

Applying the sequence component network for a LG (Line to Ground) fault:

If the bus voltage is  $V_a, V_b,$  and  $V_c$  for the 3 phases of the bus:

$$V_a = I_a^1 Z_1 + I_a^2 Z_2 + I_a^0 Z_0 \quad (1)$$

or

$$V_a = \left( I_a + \frac{Z_0 - Z_1}{Z_1} I_a^0 \right) Z_1 \quad (2)$$

Where  $V$  is the bus Voltage,  $I$  is line current and  $Z$  is the Line Impedance.

The subscripts and superscripts 1, 2, and 3 are the positive, negative and zero sequence values respectively.

Subscripts a, b and c are the values for Lines a, b and c respectively.

Hence, the impedance seen by the relay,  $Z_{seen}$  is given as:

$$Z_{seen} = \frac{V_a}{I_a + \frac{Z_0 - Z_1}{Z_1} I_a^0} \quad (3)$$

Equation (3) can be written as:

$$Z_{seen}^{AG} = \frac{V_a}{I_a + K_0 I_a^0} = \frac{V_a^0 + V_a^1 + V_a^2}{I_a + K_0 I_a^0} \quad (4)$$

Where  $Z_{seen}^{AG}$  is the impedance seen by the relay for a Line A to Ground fault, and  $K_0$  is given as:

$$K_0 = \frac{Z_0 - Z_1}{Z_1} \quad (5)$$

Similar to Equation (4), for faults involving line 'b' and 'c' to ground, the impedance seen by the relay are  $Z_{seen}^{BG}$  and  $Z_{seen}^{CG}$  respectively and they are given as:

$$Z_{seen}^{BG} = \frac{V_b}{I_b + K_0 I_b^0} = \frac{V_b^0 + V_b^1 + V_c^2}{I_b + K_0 I_b^0} \quad (6)$$

$$Z_{seen}^{CG} = \frac{V_c}{I_c + K_0 I_c^0} = \frac{V_c^0 + V_c^1 + V_c^2}{I_c + K_0 I_c^0} \quad (7)$$

Again applying the sequence components for a LL (Line to Line) fault between 'a' and 'b', the potential between lines 'a' and 'b' is  $V_a - V_b$  and the resultant current between the lines is  $I_a - I_b$ .

Then the impedance seen by the relay is:

$$Z_{seen} = \frac{V_a - V_b}{I_a - I_b} \quad (8)$$

Taking Kirchoff's voltage law (KVL) from bus 1 to bus 2 as shown in Figure 1, Equation 8 can be expanded to give the impedance seen for fault between Linea A and B,  $Z_{seen}^{AB}$  as:

$$Z_{seen}^{AB} = \frac{V_a^1 + V_a^2 - a^2 V_a^1 - a V_a^2}{I_a^1 + I_a^2 - a^2 V_a^1 - a I_a^2} \quad (9)$$

Similarly, for LL fault between 'b' and 'c', the impedance seen is  $Z_{seen}^{BC}$  and it's given as:

$$Z_{seen}^{BC} = \frac{V_b - V_c}{I_b - I_c} = \frac{V_a^1 - V_a^2}{I_a^1 - I_a^2} \quad (10)$$

And for fault between phases 'a' and 'c', the impedance seen is  $Z_{seen}^{AC}$  and given as:

$$Z_{seen}^{AC} = \frac{V_a - V_c}{I_a - I_c} = \frac{V_a^1(1-a) + V_a^2(1-a^2)}{I_a^1(1-a) - I_a^2(1-a^2)} \quad (11)$$

For a LLG (double line to ground) fault between lines 'b' and 'c' to ground and applying the sequence components on Figure 1, and the fault current that flows in the lines 'b' and 'c' (combined) to ground is

$$I_b + I_c = I_a^0 + a^2 I_a^1 + a I_a^2 + I_a^0 + a I_a^1 + a^2 I_a^2 \quad (12)$$

since  $1 + a + a^2 = 0$ , rewrite Equation (14) as:

$$I_b + I_c = 2I_a^0 - (I_a^1 + I_a^2) \quad (13)$$

Hence, the impedance seen by the relay for faults between Lines B and C to Ground,  $Z_{seen}^{BCG}$  is given as:

$$Z_{seen}^{BCG} = \frac{V_b(\text{or } V_c)}{I_b + I_c} = \frac{V_a^0 + a^2 V_a^1 + a V_a^2}{2I_a^0 - (I_a^1 + I_a^2)} = \frac{V_a^0 + a V_a^1 + a^2 V_a^2}{2I_a^0 - (I_a^1 + I_a^2)} \quad (14)$$

In same way, for lines 'a' and 'c' to ground,  $Z_{seen}^{ACG}$  is given as:

$$Z_{seen}^{ACG} = \frac{V_a(\text{or } V_c)}{I_a + I_c} = \frac{V_a^0 + V_a^1 + V_a^2}{2I_a^0 - a^2 I_a^1 - a I_a^2} = \frac{V_a^0 + a V_a^1 + a^2 V_a^2}{2I_a^0 - a^2 I_a^1 - a I_a^2} \quad (15)$$

Lines 'a' and 'b' to ground, impedance seen,  $Z_{seen}^{ABG}$  is:

$$Z_{seen}^{ABG} = \frac{V_a(\text{or } V_b)}{I_a + I_b} = \frac{V_a^0 + V_a^1 + V_a^2}{2I_a^0 - a I_a^1 - a^2 I_a^2} = \frac{V_a^0 + a^2 V_a^1 + a V_a^2}{2I_a^0 - a I_a^1 - a^2 I_a^2} \quad (16)$$

For faults involving all 3 phases, (whether all three phase to ground or clear off ground) the impedance seen by the relay,  $Z_{seen}^{ABC(G)}$  is simply:

$$Z_{seen}^{ABC(G)} = \frac{V_a^1}{I_a^1} \quad (17)$$

## 2.2. Test Network for the Study

To investigate this research, a 33 kV distribution power line shown in Figure 2 will be used to test the models developed in the previous section. The distance protection of the line has 3 protection zones – 1, 2 and 3. Zone 1 gives instantaneous protection to 80 % of Line 1 (i.e., 80 % of 73 km) while Zone 2 acts as a backup to Zone 1, also protect the remaining 20 % Line 1 and 20 % of Line 2 (i.e, Line 1's 73 km and 20 % of Line 2's 116 km) after a time delay. Lastly, Zone 3 acts as backup to Zones 1 and 2 and also protects the left 40 % of Line 2 (i.e, 100 % of Line 1 and 40 % of Line 2) after a further time delay. The line parameters are presented in Table 2.

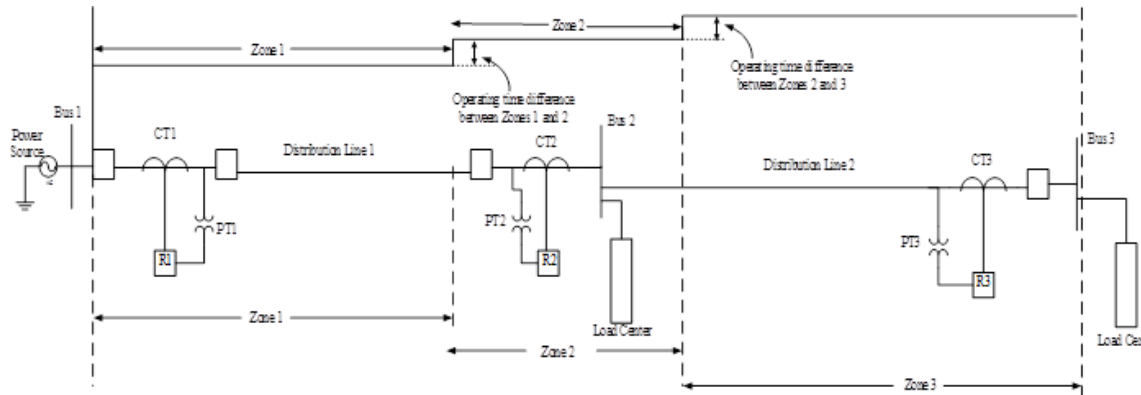


Figure 2: A 3 – Zones distance protection of a distribution line

Table 1: Line parameters

Parameter	Value
Length of Line 1	73 km
Length of Line 2	116 km
Line positive sequence resistance (same as negative sequence)	$0.02582 \times 10^{-3}(\Omega/\text{m})$
Line positive sequence reactance (same as negative sequence)	$0.1291 \times 10^{-3}(\Omega/\text{m})$
Line positive sequence capacitance (same as negative sequence)	$210.10(\Omega/\Omega^{-1})$
Line zero sequence resistance	$0.1365 \times 10^{-3}(\Omega/\text{m})$
Line zero sequence reactance	$1.021 \times 10^{-3}(\Omega/\text{m})$
Line zero sequence capacitance	$423.251710(\Omega/\Omega^{-1})$
Fault impedance used	Fault ON resistance 10 $\Omega$
	Fault OFF resistance 1.0E6 $\Omega$
K	$6.826 \angle 4.23^\circ$
Zone 1 (One)	0.0 km to 58.4 km
Zone 2 (Two)	58.41 km to 96.2 km
Zone 3 (Three)	96.21 km to 119.4 km

## 2.3. Test Network Model in PSCAD

Using Equations 4, 6, 7, 10, 11, 12, 16, and 17, the model of the DPS of the system shown in Figure 2 in PSCAD is done in as represented in the block diagram shown in Figure 3.

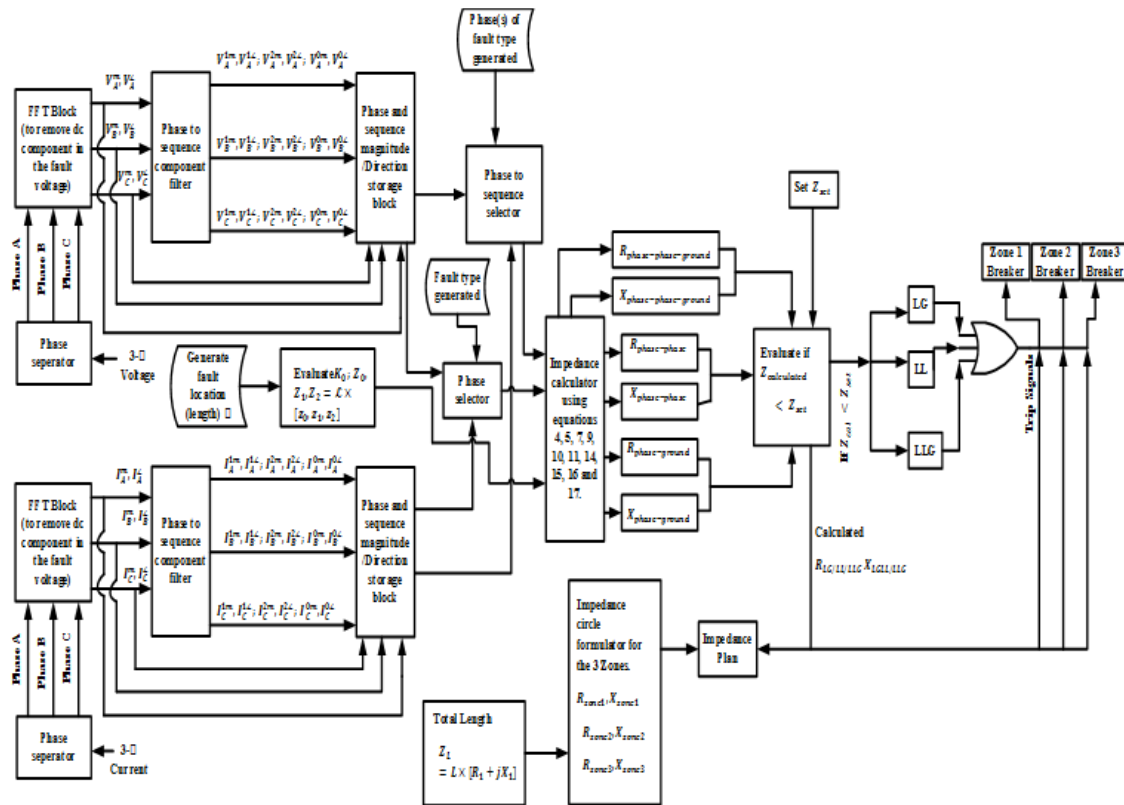


Figure 3: Block diagram of PSCAD model

### 3. RESULTS AND DISCUSSION

We shall investigate the DPS behavior using fault impedance values of 0.1 Ω, 1 Ω 5 Ω and 10 Ω for LG, LL, LLG and 3 phase faults between different lines to see how variations in fault impedance and type affect the tripping zones for faults occurring at different locations. Consider introducing different LG with different fault impedances at 50 km on Line 1 (Zone 1), the tripping of the CB and the tripping Zone for some LG fault and impedances are shown in Figure 4 and Figures 5a to 5e respectively. Also, by introducing different faults with different fault impedances at 40 km on Line 2 (Zone 3), the tripping zones for some of the fault and impedances are shown in Figure 6a to 6d. Figure 6e and 7 shows that the system does not trip for that particular fault with impedance as its reach for that particular fault is beyond the reach of the system.

Some results of the protective behavior of the DPS for the 33 kV system under analysis for different types of faults across different phases and to ground and for different fault impedance occurring at selected locations are presented in Table 2.

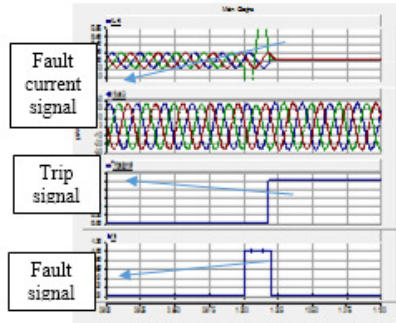


Figure 4: V, I, Fault & Trip signal waveform

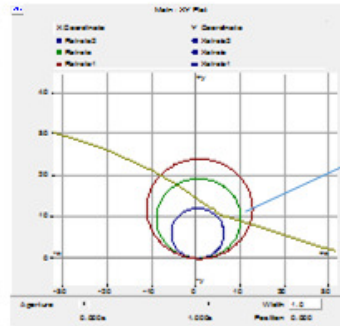


Figure 5a: LG (CG) 0.1 Ω fault

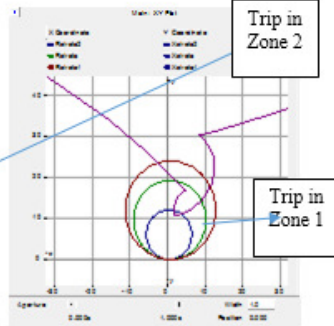


Figure 5b: LG (BG) 0.1 Ω fault

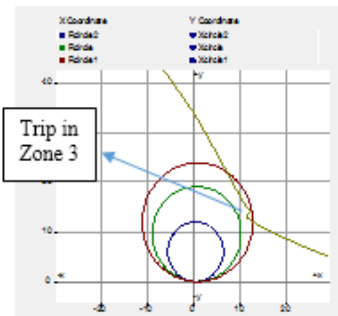


Figure 5c: LG (CG) 5 Ω fault

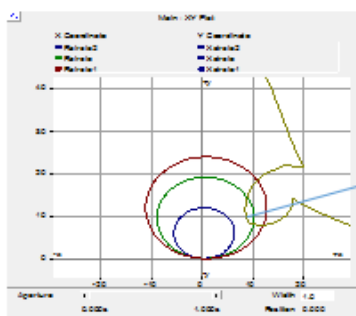


Figure 5d: LG (CG) 5 Ω fault

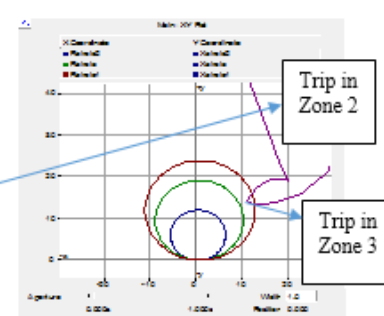


Figure 5e: LG (CG) 5 Ω fault

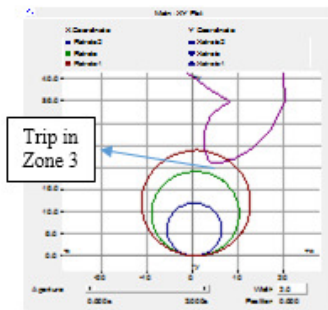


Figure 6a: LG (BG) fault of 5 Ω

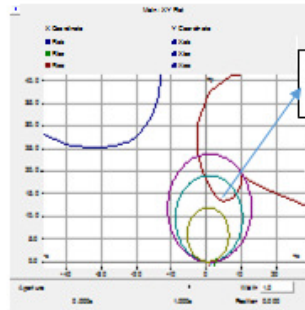


Figure 6b: LL (AC) fault of 5 Ω

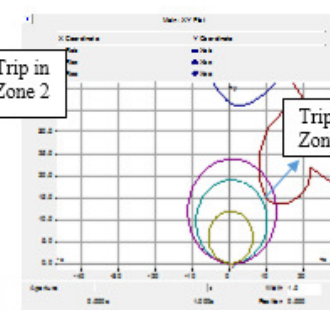


Figure 6c: 10 Ω LLG (ABG) fault

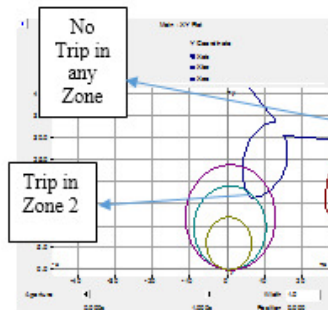


Figure 6d: 5 Ω LLG (ABG) fault

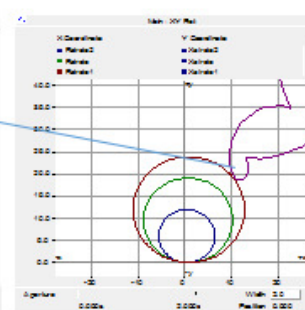


Figure 6e: 10 Ω LG (BG) fault

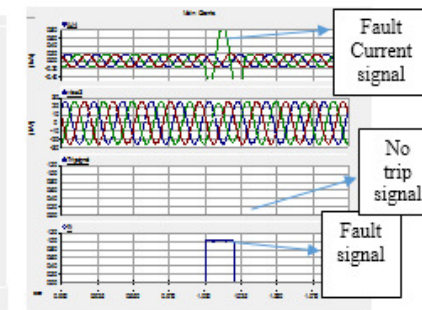


Figure 7: V, I, Fault & Trip signal waveform

Table 2: Tripping zones for different faults with different fault impedance

S/N	Fault location	Fault resistance (Ω)	Fault type	Trip zone	S/N	Fault location	Fault resistance (Ω)	Fault type	Trip zone
1	50 km on Line 1 (Zone 1)	0.1 Ω	LG (AG)	Zone 2	2	50 km on Line 1 (Zone 1)	1.0 Ω	LG (AG)	Zone 2
			LG (BG)	Zone 1				LG (BG)	Zone 1
			LG (CG)	Zone 2				LG (CG)	Zone 2
			LL (AB)	Zone 2				LL (AB)	Zone 2
			LL (AC)	Zone 1				LL (AC)	Zone 1
			LL (BC)	Zone 1				LL (BC)	Zone 1
			LLG (ABG)	Zone 2				LLG (ABG)	Zone 2
			LLG (ACG)	Zone 1				LLG (ACG)	Zone 2
			LLG (BCG)	Zone 1				LLG (BCG)	Zone 2
			3 Phase	Zone 1				3 Phase	Zone 2
2	50 km on Line 1 (Zone 1)	5.0 Ω	LG (AG)	Zone 2	4	50 km on Line 1 (Zone 1)	10.0 Ω	LG (AG)	Zone 2
			LG (BG)	Zone 2				LG (BG)	Zone 3
			LG (CG)	Zone 3				LG (CG)	Zone 2
			LL (AB)	Zone 3				LL (AB)	Zone 2
			LL (AC)	Zone 2				LL (AC)	Zone 3
			LL (BC)	Zone 1				LL (BC)	Zone 3
			LLG (ABG)	Zone 2				LLG (ABG)	Zone 2
			LLG (ACG)	Zone 2				LLG (ACG)	Zone 2
			LLG (BCG)	Zone 1				LLG (BCG)	Zone 3
			3 Phase	Zone 1				3 Phase	Zone 2
3	18 km on Line 2 (Zone 2)	0.1 Ω	LG (AG)	Zone 3	6	18 km on Line 2 (Zone 2)	1.0 Ω	LG (AG)	Zone 2
			LG (BG)	Zone 2				LG (BG)	Zone 2
			LG (CG)	Zone 3				LG (CG)	Zone 3
			LL (AB)	Zone 2				LL (AB)	Zone 2
			LL (AC)	Zone 2				LL (AC)	Zone 2
			LL (BC)	Zone 2				LL (BC)	Zone 3
			LLG (ABG)	Zone 2				LLG (ABG)	Zone 3
			LLG (ACG)	Zone 2				LLG (ACG)	Zone 2
			LLG (BCG)	Zone 2				LLG (BCG)	Zone 2
			3 Phase	Zone 2				3 Phase	Zone 2
4	18 km on Line 2 (Zone 2)	5.0 Ω	LG (AG)	Zone 2	8	18 km on Line 2 (Zone 2)	10.0 Ω	LG (AG)	Zone 3
			LG (BG)	Zone 3				LG (BG)	Zone 3
			LG (CG)	Zone 2				LG (CG)	Zone 3
			LL (AB)	Zone 2				LL (AB)	Zone 2
			LL (AC)	Zone 3				LL (AC)	Zone 2
			LL (BC)	Zone 2				LL (BC)	Zone 2
			LLG (ABG)	Zone 2				LLG (ABG)	Zone 3
			LLG (ACG)	Zone 2				LLG (ACG)	Zone 3
			LLG (BCG)	Zone 2				LLG (BCG)	Zone 3
			3 Phase	Zone 2				3 Phase	Zone 3
5	40 km on Line 2 (Zone 3)	5.0 Ω	LG (AG)	Zone 3	10	40 km on Line 2 (Zone 3)	10.0 Ω	LG (AG)	Zone 3
			LG (BG)	Zone 3				LG (BG)	No trip
			LG (CG)	Zone 3				LG (CG)	Zone 3
			LL (AB)	Zone 2				LL (AB)	Zone 2
			LL (AC)	Zone 2				LL (AC)	Zone 2
			LL (BC)	Zone 3				LL (BC)	Zone 3
			LLG (ABG)	Zone 2				LLG (ABG)	Zone 3
			LLG (ACG)	Zone 2				LLG (ACG)	Zone 3
			LLG (BCG)	Zone 2				LLG (BCG)	Zone 3
			3 Phase	Zone 3				3 Phase	Zone 3

Let an accurate trip location of the relay be TripP and inaccurate trip location of the relay be TripQ. Total test carried out was 250, total accurate trip, TripP = 163, total inaccurate trip, TripQ = 87. Hence, the sum of the sum of the accurate and inaccurate trips are given as:

$$\sum_{i=1}^{250} TripP_i + \sum_{i=1}^{250} TripQ_i = 250 \quad (18)$$

The percentage accuracy of the protection scheme can be calculated as:

$$\% \text{ accuracy} = \frac{\sum_{i=1}^{250} TripP}{250} \times 100 = 62.5 \% \quad (19)$$



From the results recorded from the simulations carried out for an impedance fault of  $0.1 \Omega$  at 50 km on Line 1, different types of faults trips in different zones. A line 'A' to ground fault (AG) trips inaccurately at Zone 2 while for a BG fault, the trips accurately at Zone 1. Also, line 'A' to line 'C' fault at the same location of 50 km on Line 1 trips at Zone 1 for fault impedances of  $0.1 \Omega$  and  $1 \Omega$ . The same fault at the same location across the same line trips in Zone 2 and Zone 3 for fault impedance of  $5 \Omega$  and  $10 \Omega$  respectively.

For a  $5 \Omega$  LG (BG) fault that occurred at 40 km on Line 2 (Zone 3), the simulation shows that the DSP trips at Zone 2. However, for same type of fault at the same location and of  $10 \Omega$  impedance, the simulation in PSCAD shows no tripping in any of the zones as shown in Fig. 11e and 12. In this instance, the impedance seen by the distance relay of the DPS is slightly beyond the set impedance. However, for a for  $5 \Omega$  and  $10 \Omega$  LL fault occurring at 40 km on Line 2 fault between lines 'B' and 'C', the DPS trip accurately at Zone 3. The average tripping zone accuracy of the distance relay for the 33 kV network tested is 62.5%.

#### 4. CONCLUSION

When a fault occurs in a system protected by the DPS, the zone where the tripping of the CB takes place is not solely dependent on the location where the fault occur as it is ideally thought to be. This research has shown that the trip location depends on:

- (i) The location of the fault.
- (ii) The fault impedance.
- (iii) The type of fault and
- (iv) The phase or phases involved in the fault.

#### 5. ACKNOWLEDGMENT

The authors wish to acknowledge the assistance of the staffs of EEDC (Enugu Electricity Distribution Company) for suppling us with distribution line data needed for this research.

#### 6. CONFLICT OF INTEREST

There is no conflict of interest associated with this work.

#### REFERENCES

- Adhikari, S. and Sinha, N. (2016). Optimal Coordination of Directional Overcurrent Relays Using Bacteria Foraging Algorithm. *Journal of Scientific and Industrial Research*, 75 (7), pp. 557 – 561.
- Bedekar, P. P. Bhide, S. R. and Kale, V. S. (2010). Optimum Coordination of Overcurrent Relay Timing Using Simplex Method. *Electric Power Components and Systems*, 38, pp. 1175 – 1193.
- Benmouyal, G.; Fischer, N.; Guzman, A.; Mooney, J. and Tziouvaras, D. (2004). Advanced transmission line protection system. 8<sup>th</sup> IEE International Conference on Developments in Power System Protection, Amsterdam, Netherlands, 2, pp. 445 – 448.
- Ghanizadeh, T. B., Seyedi, H., Hashemi, S. M. and Nezhad, P. S. (2015). Impedance – Differential Protection: A New Approach to Transmission – Line Pilot Protection. *IEEE Transactions on Power Delivery*, 30 (6), pp. 2510 – 2518.
- Hashemi, S. M., Tarafdar, H. M. and Seyedi, H. (2013). Transmission-Line Protection: A Directional Comparison Scheme Using the Average of Superimposed Components. *IEEE Transactions on Power Delivery*, 28 (2), pp. 955 – 964.
- Huanhuan, W., Song, G., Ding, J. and Yang, L. (2014). Long line distance protection based on fast phasor calculation algorithm. 12<sup>th</sup> IET International Conference on Developments in Power System Protection (DPSP 2014), Copenhagen, Denmark, pp. 46 – 57.
- Masoud, M. E. and Mahfouz, M. M. A. (2010). Protection scheme for transmission lines based on alienation coefficients for current signals. *IET Generation, Transmission and Distribution*, 4 (11), pp. 1236 – 1244.
- Murthy, P. S. R. (2007). Power system analysis. B.S Publication, 4-4-309, Giriraj Lane, Sultan Bazar.

- Noghabi, A. S.; Sadeh, J. and Mashhadi, H. R. (2009). Considering Different Network Topologies in Optimal Overcurrent Relay Coordination Using a Hybrid GA. *IEEE Transactions on Power Delivery*, 24, pp. 1857 – 1863.
- Onwuka, I. K, Oputa, O, Diyoke, G. C, Ezeonye, C. S and Obi, P. I. (2023). Effects of varying fault impedance on distance protection schemes of 11 kv distribution systems. *Beyero Journal of Engineering and Technology*, 18(2), pp. 71 – 83.
- Pragati, B. A. and Amol, K. A. (2017). Optimum Coordination of Overcurrent and Distance Relays Using JAYA Optimization Algorithm. 2017 International Conference on Nascent Technologies in the Engineering Field, Navi Mumbai, India, 1 – 5.
- Suonan, J., Wang, L. and Xia, J. (2010). Harmonic Analysis of Fault Signal in UHV Transmission Line. *High Voltage Engineering Journal*, 36 (1), pp. 37 – 43.
- Tohid, G. B., Seyed, H. and Hashemi, S. M. (2014). Protection of transmission lines using fault component integrated power. *IET Generation, Transmission and Distribution*, 8 (12), pp. 2163 – 2172.
- Verma, M. and Sinha, A. (2016). Implementation of quadrilateral relay for three zone protection of transmission line. 7<sup>th</sup> India International Conference on Power Electronics (IICPE), Patiala, India, 17 – 19.
- Wadood, A., Farkoush, S. G., Khurshaid, T., Kim, C., Yu, J., Geemand, Z. W. and Rhee, S. (2018). An Optimized Protection Coordination Scheme for the Optimal Coordination of Overcurrent Relays Using a Nature-Inspired Root Tree Algorithm. *Applied Science Journal*, 8 (1664), pp. 1 – 22.